Journal of Organometallic Chemistry, 429 (1992) 143–152
Elsevier Sequoia S.A., Lausanne
JOM 22427

Reaction of organocalcium and -barium complexes with pyrazines. X-ray structural characterization of $[(Me_5C_5)_2Ba]_2(\mu\text{-}C_4H_4N_2)$

R. Allen Williams, Timothy P. Hanusa
Department of Chemistry, Vanderbilt University, Nashville, TN 37235 (USA)

and John C. Huffman
Molecular Structure Center, Department of Chemistry, Indiana University, Bloomington, IN 47405 (USA)

(Received August 19, 1991)

Abstract

Bis(pentamethylcyclopentadienyl)calcium and -barium react in toluene with pyrazine and 2,3,5,6-tetramethylpyrazine to form highly colored adducts. Spectroscopic studies reveal that a concentration-dependent mononuclear–binuclear equilibrium exists for the $[Cp^*_2Ca]_2(\mu\text{-}C_4Me_4N_2)$ adduct ($Cp^* = Me_5C_5$). A bimetallic structure was confirmed in the solid state for $[Cp^*_2Ba]_2(\mu\text{-}C_4H_4N_2]$ by X-ray diffraction. The complex crystallizes from toluene in the monoclinic space group $P2_1/n$, with $a = 15.203(2)$, $b = 11.083(2)$, $c = 26.436(5)$ Å, $\beta = 103.48(1)°$ and $D_c = 1.37$ g cm^{-3} for $Z = 4$ (complexes). Least-squares refinement based on 4259 observed reflections measured at −155°C led to a final R value of 0.068. Two independent pyrazine-bridged binuclear complexes appear in the asymmetric cell, each with a crystallographically imposed center of inversion. Each barium in the $[Ba_2(\mu\text{-}C_4H_4N_2)]_2$ core is flanked by two $(\eta^5\text{-}Cp^*)$ rings with average Ba–C distances in both complexes of 2.96(1) Å; the Ba–N distances in the two complexes are 2.867(7) Å and 2.937(6) Å, respectively.

Introduction

Metal complexes containing aromatic nitrogen heterocycles have proven to be versatile probes for studies of charge transfer, electron transport [1,2], and magnetic superexchange phenomena [3,4]. Compounds containing *d*-block, and to a lesser extent *f*-block metals [5,6], have received considerable attention for these purposes. Main-group compounds with heterocyclic ligands have also been explored, as many of them exhibit intense charge transfer spectra [7,8] or unusual structural features [9].

Correspondence to: Dr. T.P. Hanusa, Department of Chemistry, Vanderbilt University, Nashville, TN 37235, USA.

Our interest in the organometallic compounds of the calcium subgroup metals [10–14] has led us to examine their adducts with a variety of aromatic nitrogen heterocycles. Although 2,2′-bipyridine adducts of Cp^*_2Ca, Cp^*_2Sr, and Cp^*_2Ba ($Cp^* = Me_5C_5$) have been prepared as intensely colored orange–red solids [15], they have only limited solubility, and no NMR or structural data have been reported for them. We were particularly interested in preparing pyrazine adducts of organoalkaline-earth compounds, as pyrazine has proven to be an unusually flexible heterocyclic ligand; it can adopt both terminal [2] and bridging [1,3] bonding modes, and can serve as a link in organometallic polymers [16–19]. Its complexes, both main-group and transition metal, often possess unusual optical and electronic properties [20,21]. We report here the synthesis and spectroscopic characterization of pyrazine adducts of Cp^*_2Ca and Cp^*_2Ba, and the crystallographic characterization of one of the latter.

Experimental

All manipulations were performed with the rigid exclusion of air and moisture. Chemicals were handled using high vacuum or Schlenk techniques, or in a Vacuum Atmospheres HE-143 drybox equipped with an MO40-1 recirculating purifier. ^1H NMR spectra were obtained at 300 MHz with a Bruker NR-300 spectrometer and were referenced to the residual proton resonances of C_6D_6 (δ 7.15); carbon (^{13}C) NMR spectra were recorded at 50.3 MHz on a Bruker NR-200 spectrometer and were referenced to the residual ^{13}C resonances of C_6D_6 (δ 128.0). Infrared data were obtained on a Perkin–Elmer 1430 spectrometer; the KBr pellets were prepared as previously described [22]. Melting points were obtained in sealed capillaries under nitrogen and are uncorrected. Elemental analyses were performed by Analytische Laboratorien, Engelskirchen, Germany.

Materials

Cp^*_2Ae (Ae = Ca, Ba) were prepared from the reaction of KCp^* and AeI_2 in diethyl ether or THF, and treated as previously described to remove coordinated solvent [10,14]. Pyrazine and 2,3,5,6-tetramethylpyrazine (Aldrich) were used as received. Solvents for reactions were distilled under nitrogen from sodium or potassium benzophenone ketyl. NMR solvents were stirred over sodium or potassium and vacuum transferred before use.

UV–vis spectroscopy

Spectra were run in 2 cm quartz cuvettes with Teflon stoppers on a Cary 2300 UV–vis spectrophotometer at 25°C. Stock solutions of the metallocenes (0.03 M) and pyrazines (0.2 M) were prepared in toluene. The samples were made by taking 1 mL aliquots of the pyrazine solutions, diluting them to 10 mL with toluene, repeating the dilution with another 10 mL of toluene, then finally diluting 1 mL aliquots of the resulting solution to 10 mL with the metallocene stock solution. The resulting concentration of pyrazine was 2.0×10^{-4} M in a solution that was 2.7×10^{-2} M in metallocene. The 140-fold excess of the metallocene was used to suppress dissociation of the complex, so that the concentration of the complex could be assumed to be equal to that of the pyrazine. The reference cell was filled with a 2.7×10^{-2} M solution of the appropriate metallocene. The absorption due to Cp^*_2Ba (see below) is sufficiently intense that the effective cutoff point for solutions of organobarium complexes is near 415 nm.

Preparation of pyrazine adducts

The adducts were formed by the addition of the decamethylmetallocenes to pyrazine or tetramethylpyrazine in toluene; removal of the solvent left the adducts in quantitative yield. Details are given for $[Cp^*_2Ca]_2(\mu\text{-}C_4H_4N_2)$; the others were formed similarly.

Synthesis of $[Cp^*_2Ca]_2(\mu\text{-}C_4H_4N_2)$. Cp^*_2Ca (0.311 g, 1.00 mmol) was added to a solution of pyrazine (0.040 g, 0.50 mmol) in toluene (25 mL). The solution immediately turned dark red and then purple. The reaction was stirred overnight, after which evaporation of the solvent left 0.350 g (quant. yield) of a dark purple solid. The complex crystallizes on cooling of a saturated boiling toluene solution as small dark purple crystals, m.p. > 300°C. Anal. Calc. for $C_{44}H_{64}Ca_2N_2$: C, 75.37; H, 9.20; Ca, 11.43; N, 4.00. Found: C, 67.52; H, 8.27; Ca, 9.41; N, 3.42%. Evidently the combustion was not as complete as possible, a situation previously observed in other alkaline-earth systems [12,23]. The observed Ca/N molar ratio of 1.0, however, confirms the expected stoichiometry for the adduct. ^1H NMR (C_6D_6, 4.3 mg mL^{-1}, 20°C): δ 7.45 (s, 4H, $C_4N_2H_4$); 1.92 (s, 60H, Cp*). Major IR bands (KBr pellet, cm^{-1}): 2850vs, br, 2725m, sh, 1438s, br, 1414s, br, 1258w, br, 1151w, 1108w, 1048m, sh, 1015w, 802m, 670w, 608br, 457m, sh, 360s, br, 290w. UV–vis: in the presence of excess metallocene (see above), λ_{max} is 535 nm and ϵ_{max} is 5500 L mol^{-1} cm^{-1}.

Synthesis of $[Cp^*_2Ca]_2(\mu\text{-}2,3,5,6\text{-}(CH_3)_4C_4N_2)$. The complex crystallizes from hot toluene as well-formed red prisms, dec. 320–325°C. Anal. Calc. for $C_{48}H_{72}Ca_2N_2$: C, 76.13; H, 9.58; Ca, 10.59; N, 3.70. Found: C, 67.52; H, 8.27; Ca, 9.41; N, 3.42%. As with the pyrazine adduct, the analysis appears incomplete; the Ca/N ratio is again 1.0, however, in agreement with the proposed stoichiometry. ^1H NMR (C_6D_6, 20°C): δ 1.90 (s, 12H, $C_4N_2Me_4$); 1.96 (s, 30H, Cp*). Major IR bands (KBr pellet, cm^{-1}): 2850vs, br, 1430s, br, 1370m, 1238sh, 1218sh, 1180m, 1010w, 986w, 810w, 800vw, 475w, 337s. UV–vis: in the presence of excess metallocene (see above), λ_{max} is 469 nm and ϵ_{max} is 4900 L mol^{-1} cm^{-1}.

Synthesis of $[Cp^*_2Ba]_2(\mu\text{-}C_4H_4N_2)$. The complex crystallizes from a hot 1:1 toluene/heptane mixture as well-formed brick-red prisms, m.p. 226–227°C. Anal. Calc. for $C_{44}H_{64}Ba_2N_2$: C, 59.00; H, 7.20; Ba, 30.67; N, 3.13. Found: C, 58.57; H, 7.22; Ba, 30.85; N, 3.03%. ^1H NMR (C_6D_6, 7 mg mL^{-1}, 20°C): δ 7.85 (s, 4H, $C_4N_2H_4$); 1.97 (s, 30H, Cp*). Major IR bands (KBr pellet, cm^{-1}): 2850vs, br, 1434m, br, 1404s, sh, 1255w, 1137m, 1108m, 1075w, 1033m, sh, 797m, 426m. UV–vis: in the presence of excess metallocene (see above), λ_{max} is 440 nm and ϵ_{max} is 438.5 L mol^{-1} cm^{-1}.

Synthesis of $[Cp^*_2Ba]_2(\mu\text{-}2,3,5,6\text{-}(CH_3)_4C_4N_2)$. The complex crystallizes on cooling from hot toluene solutions as small orange prisms. The compound darkens above 287°C, but melting does not occur below 325°C. Anal. Calc. for $C_{48}H_{72}Ba_2N_2$: C, 60.57; H, 7.63; Ba, 28.86; N, 2.94. Found: C, 60.43; H, 7.24; Ba, 28.70; N, 2.87%. ^1H NMR (C_6D_6, 20°C): δ 1.97 (s, 30H, Cp*); 2.09 (s, 12H, $C_4N_2Me_4$). Major IR bands (KBr pellet, cm^{-1}): 2850vs, br, 1430s, 1410s, 1375m, 1220sh, 1202sh, 1170m, 1010w, 986w, 795w, 452w. UV–vis: no maximum value was observed before solution cutoff of 415 nm.

Table 1

Crystal data and summary of data collection for $[Cp^{*}{}_2Ba]_2(\mu\text{-}C_4H_4N_2)$

Formula	$C_{44}H_{64}Ba_2N_2$	Wavelength (Å)	0.71069 Å
F_w	895.67	Abs. coeff. (cm^{-1})	18.351
Color of crystal	yellow	Type of scan	continuous θ–2θ
Crystal dimensions (mm)	$0.25 \times 0.25 \times 0.25$	Scan speed (deg min^{-1})	4.0
Space group	$P2_1/n$	Scan width	1.8 + dispersion
Cell dimensions (at −155°C; 60 reflections)		Background counting	6 s at extremes of scan
a (Å)	15.203(2)	Limits of data collection	$6° \leq 2\theta \leq 45°$
b (Å)	11.083(2)	No. of unique intensities	5652
c (Å)	26.436(5)	No. with $F > 2.33\sigma(F)$	4259
β (deg)	103.48(1)	$R(F)$	0.068
V ($Å^3$)	4332(2)	$R_w(F)$	0.062
Z (complexes/cell)	4	Goodness of fit	1.124
D (calc.) (g cm^{-3})	1.373	Max Δ/σ in final cycle	0.45

X-ray crystallography of $[Cp^{*}{}_2Ba]_2(\mu\text{-}C_4H_4N_2)$

General procedures for data collection and reduction have been described previously [24]. A suitable yellow crystal measuring $0.25 \times 0.25 \times 0.25$ mm^3 was located and transferred using standard inert atmosphere techniques to a Picker four-circle goniostat equipped with a Furnas Monochromator (HOG crystal) and Picker X-ray generator. The crystal was cooled to −155°C for characterization and data collection. Relevant crystal and data collection parameters for the present study are given in Table 1.

A systematic search of a limited hemisphere of reciprocal space located a set of diffraction maxima with symmetry and systematic absences corresponding to the unique monoclinic space group $P2_1/n$ (alternate setting of $P2_1/c$, No. 14). Subsequent solution and refinement of the structure confirmed this choice. A calculated density of 1.373 for $Z = 4$ indicated one complete molecule in the asymmetric unit.

Data collection was performed using standard moving-crystal/moving-detector techniques with fixed backgrounds. Data were reduced to a unique set of intensities and associated sigmas in the usual manner. The structure was solved by a combination of direct methods (MULTAN78) and Fourier techniques, using locally modified versions of the Los Alamos Crystallographic Program Library. Two independent halves of bimetallic complexes were located in the asymmetric unit. A difference Fourier synthesis revealed the location of some, but not all, hydrogen atoms. All hydrogen atom positions were therefore calculated using idealized geometries and $d(C\text{–}H) = 0.95$ Å. These calculated positions were fixed for the final cycles of refinement. Positional parameters are supplied in Table 2; selected bond distances and angles are listed in Table 3.

Results and discussion

Synthesis of pyrazine adducts

The unsolvated decamethylmetallocenes $Cp^{*}{}_2Ca$ and $Cp^{*}{}_2Ba$ react instantly on mixing with pyrazine and 2,3,5,6-tetramethylpyrazine in toluene to yield deep

Table 2

Fractional coordinates (×10^4) and isotropic thermal parameters (×10 $Å^2$) for the non-hydrogen atoms in $[Cp^*{}_2Ba]_2(\mu\text{-}C_4H_4N_2)$

Atom	*x*	*y*	*z*	B_{iso} [a]
Ba(1)	1957.0(4)	1550(1)	1248.7(3)	19
N(2)	611(7)	570(12)	404(5)	32
C(3)	863(8)	31(13)	12(6)	30
C(4)	−283(9)	539(11)	399(5)	22
C(5)	2611(8)	3729(13)	825(5)	25
C(6)	3386(8)	3272(13)	1193(6)	27
C(7)	3692(8)	2255(13)	969(5)	25
C(8)	3122(8)	2034(13)	479(5)	22
C(9)	2457(8)	2993(12)	378(5)	18
C(10)	2061(8)	4749(14)	929(6)	28
C(11)	3762(9)	3803(15)	1724(6)	36
C(12)	4519(8)	1498(15)	1206(6)	32
C(13)	3275(9)	1098(15)	109(5)	31
C(14)	1763(9)	3143(15)	−127(6)	36
C(15)	2645(9)	−761(13)	1723(6)	28
C(16)	2838(9)	95(16)	2114(6)	34
C(17)	2030(9)	439(13)	2249(5)	24
C(18)	1330(8)	−213(12)	1919(5)	21
C(19)	1698(9)	−958(15)	1595(6)	31
C(20)	3316(10)	−1416(17)	1480(7)	42
C(21)	3750(10)	561(16)	2396(7)	41
C(22)	1941(10)	1383(15)	2627(6)	36
C(23)	333(9)	−149(13)	1932(6)	30
C(24)	1201(10)	−1909(13)	1232(6)	31
Ba(25)	2379.1(5)	5310(1)	8928.6(3)	20
N(26)	4134(7)	5134(11)	9679(4)	27
C(27)	4863(9)	5626(14)	9567(5)	28
C(28)	4274(8)	4507(14)	10122(5)	27
C(29)	2268(8)	7929(12)	9125(6)	22
C(30)	1606(8)	7786(12)	8655(5)	22
C(31)	874(7)	7107(13)	8786(6)	23
C(32)	1100(8)	6909(12)	9318(5)	22
C(33)	1960(9)	7417(13)	9525(5)	25
C(34)	3184(9)	8514(15)	9158(6)	36
C(35)	1653(9)	8265(15)	8129(6)	35
C(36)	−9(9)	6826(15)	8405(6)	34
C(37)	477(9)	6330(16)	9625(6)	37
C(38)	2465(10)	7371(16)	10084(6)	39
C(39)	2092(8)	4647(12)	7835(5)	19
C(40)	3054(8)	4850(12)	7994(5)	22
C(41)	3400(9)	3852(15)	8306(6)	31
C(42)	2691(11)	3092(13)	8376(6)	33
C(43)	1887(9)	3583(13)	8092(6)	26
C(44)	1428(10)	5393(16)	7448(6)	38
C(45)	3581(9)	5826(14)	7819(6)	31
C(46)	4405(11)	3555(19)	8509(8)	56
C(47)	2789(13)	1915(16)	8669(7)	49
C(48)	921(11)	3134(15)	8035(7)	42

[a] Isotropic values for those atoms refined anisotropically are calculated using the formula given by W.C. Hamilton, *Acta Crystallogr.*, 12 (1959) 609.

Table 3

Selected bond lengths and angles in $[Cp^*_2Ba)_2(\mu\text{-}C_4H_4N_2)$

Atoms	Distance (Å)	Atoms	Angle (deg)
Ba(1)–N(2)	2.867(7) [a]	C(3)–N(2)–C(4)	116.8(11) [a]
N(2)–C(3)	1.329(18) [a]	N(2)–C(3)–C(4)	124.9(11) [a]
N(2)–C(4)	1.357(17) [a]	N(2)–C(4)–C(3)	118.3(12) [a]
C(3)–C(4)	1.381(19) [a]	C(27)–N(26)–C(28)	116.0(11)
Ba(25)–N(26)	2.937(6)	N(26)–C(27)–C(28)	123.3(12)
N(26)–C(27)	1.331(17)	N(26)–C(28)–C(27)	120.8(11)
N(26)–C(28)	1.335(17)		
C(27)–C(28)	1.383(18)		
	Conformer A	*Conformer B*	
Ba–C (ring) (ave.) (Å)	2.96(2)	2.96(2)	
Ba–ring centroid (Å)	2.67, 2.73	2.68, 2.77	
C–C (ring) (ave.) (Å)	1.41(6)	1.42(6)	
C(ring)–C(methyl) (ave.) (Å)	1.50(6)	1.51(6)	
Planarity of rings	within 0.02 Å	within 0.03 Å	
Ave. displacement of CH_3 groups from ring plane	0.83 Å	0.90 Å	

[a] Refers to a value in conformer A.

orange–red to purple colored solutions. Evaporation of the solutions yields Cp^*_2Ae/pyrazine 2:1 adducts in quantitative yield as thermally stable solids. The avidity of the metallocenes for the heterocycles is remarkable; even solid Cp^*_2Ca will react with the slight amount of vapor present over pyrazine at room temperature to produce an orange adduct. Just as easily, however, the pyrazines are displaced by O-donor bases such as diethyl ether, DME and THF. Prolonged pumping under dynamic vacuum can cause loss of some pyrazine, and thus should be avoided to maintain correct stoichiometries.

UV–vis spectra

Study of the organobarium compounds by UV–vis spectroscopy is complicated by the strong UV absorbance of Cp^*_2Ba in aromatic solvents; the absorbance tails into the visible region, giving solutions of the decamethylmetallocene a deep yellow color. The absorption is intense enough that the effective solution cutoff point is near 415 nm. As solid Cp^*_2Ba is colorless, the color apparently arises from an interaction with the aromatic solvent, although no stable adducts have been isolated. Attempts to avoid the problem by studying the absorption spectra in alkanes are handicapped by the limited solubility of both Cp^*_2Ba and its pyrazine adducts in such solvents.

The pyrazine adduct of Cp^*_2Ba has a broad absorbance with a maximum at 430–440 nm, but because this value is so near the solution cutoff, it is not easily reproducible from run to run. Similarly, the ϵ_{max} value at a pyrazine concentration of 2.0×10^{-4} M is observed to vary between 440 and 600 L mol^{-1} cm^{-1}, again probably as a consequence of the nearness of the solution cutoff. No such difficulties were experienced with the calcium complexes (for the parent Cp^*_2Ca, ϵ_{max} is 4200 L mol^{-1} cm^{-1} at 269 nm).

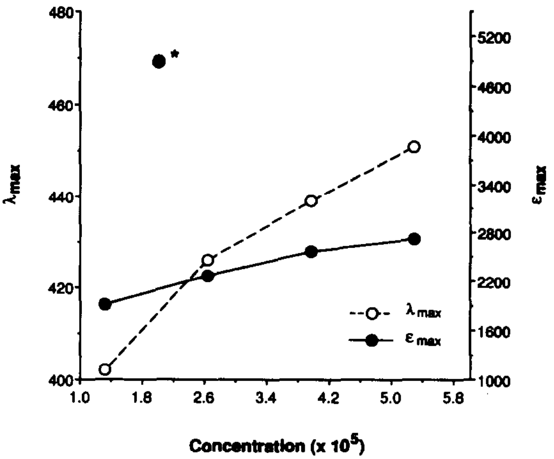

Fig. 1. UV–vis data for $[Cp^*{}_2Ca]_2(\mu\text{-}C_4Me_4N_2)$ in toluene. The outlying data point (*) was measured in the presence of a 135-fold excess of $Cp^*{}_2Ca$.

The tetramethylpyrazine adduct of $Cp^*{}_2Ca$ was chosen for the most detailed study, as it is readily crystallized and its solutions are free from the absorption problems of the barium complexes. The λ_{max} value of this complex is concentration dependent, and shifts toward higher frequencies on increasing dilution or on addition of excess pyrazine. Addition of excess metallocene causes a shift to lower frequencies (Fig. 1). The fact that the molar absorptivity varies with concentration is evidence that the absorbing species changes within the concentration range. This behavior is inconsistent with simple dilution, and suggests that dissociation is occurring.

The dissociation process was tested by experiments in which large excesses of $Cp^*{}_2Ca$ were added to the solutions. For example, by extrapolating from nearby values, an ϵ_{max} of *ca.* 2100 L mol^{-1} cm^{-1} would be expected for a solution with a tetramethylpyrazine concentration of 2.0×10^{-4} *M* (nominally equal to the adduct concentration). In the presence of a 135-fold excess of $Cp^*{}_2Ca$, however, the observed ϵ_{max} is 4900 L mol^{-1} cm^{-1}, a much higher value that may be close to that for the undissociated adduct (Fig. 1). Assuming this to be true, the "standard" λ_{max} and ϵ_{max} values for all the adducts were recorded in solutions containing an excess of the appropriate metallocene.

A single-step dissociation (*i.e.*, $[Cp^*{}_2Ca]_2(\mu\text{-}C_4Me_4N_2) \rightleftharpoons 2Cp^*{}_2Ca + C_4Me_4N_2$) in which the concentrations of the colorless $Cp^*{}_2Ca$ and $C_4Me_4N_2$ accumulate on dilution, is incompatible with the shifts observed in λ_{max}. Such changes are accommodated, however, by a two-step equilibrium process involving the dissociation of pyrazine (eqs. 1 and 2).

$$[Cp^*{}_2Ca]_2(\mu\text{-}C_4Me_4N_2) \overset{K_1}{\rightleftharpoons} Cp^*{}_2Ca(\mu\text{-}C_4Me_4N_2) + Cp^*{}_2Ca \quad (1)$$

$$Cp^*{}_2Ca(\mu\text{-}C_4Me_4N_2) \overset{K_2}{\rightleftharpoons} Cp^*{}_2Ca + C_4Me_4N_2 \quad (2)$$

Variations in the amounts of $[Cp^*{}_2Ca]_2(\mu\text{-}C_4Me_4N_2)$ (orange–red) and $Cp^*{}_2Ca(\mu\text{-}C_4Me_4N_2)$ (yellow) would account for the λ_{max} behavior. Unfortunately, the absorbances of the various species overlap sufficiently so that only a single broad peak is observed in the UV–vis spectra, and a value for the individual (or overall) equilibrium constants cannot be obtained. ^{1}H NMR spectroscopy is also not useful in this regard, since although the chemical shifts of the complexes approach the values for the free metallocenes and ligands as the concentration is decreased, no more than two peaks (for Cp* and $C_4R_4N_2$) are ever observed in the spectra.

The relative contribution of charge transfer and intraligand transitions to the color of the complexes is unknown [25]. Unfortunately, the limited range of compatible solvents and the low solubilities of the compounds severely restrict experimental investigation of this question.

Structure of $[Cp^*{}_2Ba]_2(\mu\text{-}C_4H_4N_2)$

Crystals of $[(Cp^*{}_2Ba)]_2(\mu\text{-}C_4H_4N_2)$ were grown by slow evaporation of saturated toluene solutions and studied by X-ray diffraction. Two independent bimetallic complexes (A and B) appear in the asymmetric unit, each with a crystallographically imposed center of inversion. Each barium atom is coordinated by two pentamethylcyclopentadienyl rings and a bridging pyrazine group, generating formally 7-coordinate metal centers. The chief difference between the complexes is a variation in the rotation of the pyrazine ring relative to the Cp* planes. In complex "A" the closest approach of a pyrazine hydrogen to a ring methyl group occurs between H(49) and C(13) at 2.90 Å. This is somewhat less than the sum of the van der Waals' radii for CH_3 and H (3.2 Å) [26], but in complex "B" the analogous contact occurs between H(81) and C(46) at 3.41 Å. Since both binuclear forms occur in the crystal, these differences cannot be considered chemically significant and, except where noted, only complex "A" will be discussed in detail here. An ORTEP view of complex "A" providing the numbering scheme used in the tables is displayed in Fig. 2.

The average (η^5-Cp*)–Ba distance in the complex is 2.96(2) Å, and the ring centroid–Ba–ring centroid angle is 138.0°. The geometry around the barium center is distinctly pyramidal, with the barium atom lying 0.65 Å out of the plane defined by the two ring centroids and the nitrogen of the pyrazine; the sum of the two

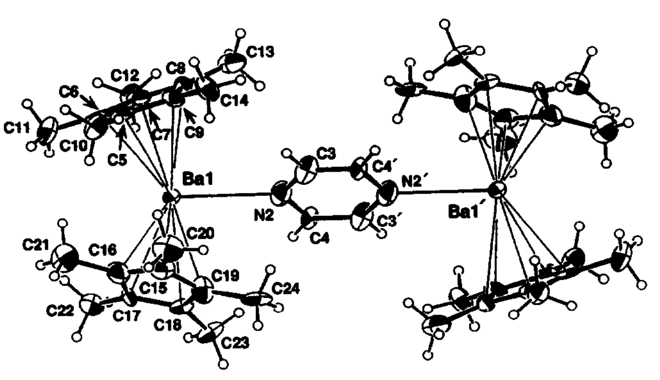

Fig. 2. ORTEP view of $[Cp^*{}_2Ba]_2(\mu\text{-}C_4H_4N_2)$ (conformer A), giving the numbering scheme used in the tables.

centroid–Ba–N angles and centroid–Ba–centroid angles is 341.5°. The average Ba–C distance is marginally, although appropriately, longer than that observed in $[(C_3H_7)_4C_5H]_2Ba$ (2.94(1) Å) [22], as the radii of 6- and 7-coordinate Ba^{2+} differ by 0.03 Å [27]. In the structure of Cp^*_2Ba, however, the average Ba–C distance is 2.99(2) Å, which is not a change in the expected direction from the bimetallic complex [11,14].

The source of this anomaly evidently lies in the structure of Cp^*_2Ba, rather than in the pyrazine complex. Subtracting the average Ba–ring centroid distances of 2.73 Å and 2.70 Å from the radii of 6- and 7-coordinate Ba^{2+} provides "Cp* radii" of 1.38 Å and 1.32 Å for Cp^*_2Ba and $[Cp^*_2Ba]_2(\mu\text{-}C_4H_4N_2)$, respectively. The former value is longer (by almost 2σ) than the mean value of the radius recently identified as characteristic of divalent cyclopentadienyl species (1.33(3) Å), whereas the value for $[Cp^*_2Ba]_2(\mu\text{-}C_4H_4N_2)$ is indistinguishable from that mean [28]. Close contacts between the rings of one metallocene and the Ba of an adjacent one probably help serve to lengthen the Ba–C(Cp*) distances in Cp^*_2Ba. The same explanation may account for the smaller ring centroid–Ba–ring centroid angle in Cp^*_2Ba (131°) than in $[Cp^*_2Ba]_2(\mu\text{-}C_4H_4N_2)$ (138°). In this case, the proximity of another Cp* ring must cause the ring angle in the metallocene to open more than the presence of a pyrazine ring.

No unusual contacts are evident in the structure: the closest non-bonded intramolecular $CH_3 \cdots CH_3'$ contact occurs between C(12) and C(21) at 3.75 Å, and the Cp* rings are planar to within 0.02 Å. The pyrazine unit is coordinated to the barium at a distance of 2.867(7) Å in complex A, and at 2.937(6) Å in complex B; these two values differ by more than 5σ, and the difference is thus statistically significant, but probably of little chemical consequence. The Ba–N $\cdots$ N' linkage is nearly linear, with an angle of 175°. The pyrazine ring is planar; the two N–C distances average 1.34(2) Å and the unique C–C' distance is 1.381(19) Å, values that are statistically indistinguishable from those in free pyrazine [29] and similar to those found in other structurally characterized complexes containing coordinated pyrazine [5,9].

If the radius suggested for 7-coordinate Ba^{2+} (1.38 Å) [27] is subtracted from the average Ba–N distance in both complexes, an "effective radius" of 1.52 Å is left for the pyrazine nitrogen atom. This value is nearly identical with that in $[Cp_3Yb]_2(\mu\text{-}C_4H_4N_2)$ (1.54 Å), which contains a similarly electropositive metal center [5]. Substantially larger radii are found in the non-ionic adduct $PCl_5 \cdot pyz$ (1.64 Å) [30], and in the tin species $(SnMe_2Cl_2)_2 \cdot pyz$ and $(SnPh_2Cl_2)_2 \cdot pyz$ (both 2.06 Å) [9]. The only smaller N radii for bridging pyrazines are found in the highly charged Creutz–Taube ions; the shortest reported to date is 1.44 Å, identified in the $\{[(NH_3)_5Ru]_2(\mu\text{-}C_4H_4N_2)\}^{6+}$ cation [31]. The relatively small value for the N radius in the organobarium and organoytterbium complexes points to the high Lewis acidity of the metals.

Conclusion

The reaction of pyrazines with alkaline-earth decamethylmetallocenes produces highly colored bridged adducts. These compounds are thermally stable, yet the pyrazines are kinetically labile, and extensive dissociation occurs in solution. Although quantification of the equilibria involved has not been possible, these complexes provide direct evidence for multistep ligand exchange processes in heavy organoalkaline-earth systems.

Acknowledgments

Acknowledgment is made to the donors of the Petroleum Research Fund, administered by the American Chemical Society, and to the Natural Science Committee of Vanderbilt University for support of this research.

References

1 C. Creutz and H. Taube, J. Am. Chem. Soc., 91 (1969) 3988.
2 C. Creutz and H. Taube, J. Am. Chem. Soc., 95 (1973) 1086.
3 H.W. Richardson, J.R. Wasson and W.E. Hatfield, Inorg. Chem., 16 (1977) 484.
4 M.S. Haddad, D.N. Hendrickson, J.P. Cannady, R.S. Drago and D.S. Bieksza, J. Am. Chem. Soc., 101 (1979) 898.
5 E.C. Baker and K.N. Raymond, Inorg. Chem., 16 (1977) 2710.
6 C.W. Eigenbrot, Jr., and K.N. Raymond, Polyhedron, 1 (1982) 417.
7 F.J.A. Des Tombe, G.J.M. van der Kerk, H.M.J.C. Creemers, N.A.D. Carey and J.G. Noltes, J. Organomet. Chem., 44 (1972) 247.
8 W. Kaim, Acc. Chem. Res., 18 (1985) 160.
9 D. Cunningham, P. McArdle, J. McManus, T. Higgins and K. Molloy, J. Chem. Soc., Dalton Trans., (1988) 2621.
10 M.J. McCormick, R.A. Williams, L.J. Levine and T.P. Hanusa, Polyhedron, 7 (1988) 725.
11 R.A. Williams, T.P. Hanusa and J.C. Huffman, J. Chem. Soc., Chem. Commun., (1988) 1045.
12 M.J. McCormick, S.C. Sockwell, C.E.H. Davies, T.P. Hanusa and J.C. Huffman, Organometallics, 8 (1989) 2044.
13 R.A. Williams, T.P. Hanusa and J.C. Huffman, J. Am. Chem. Soc., 112 (1990) 2454.
14 R.A. Williams, T.P. Hanusa and J.C. Huffman, Organometallics, 9 (1990) 1128.
15 C.J. Burns and R.A. Andersen, J. Organomet. Chem., 325 (1987) 31.
16 J. Koch and M. Hanack, Chem. Ber., 116 (1983) 2109.
17 O. Schneider and M. Hanack, Chem. Ber., 116 (1983) 2088.
18 F. Kubel and J. Straehle, Z. Naturforsch., Teil B, 36 (1981) 441.
19 J.P. Collman, J.T. McDevitt, C.R. Leidner, G.T. Yee, J.B. Torrance and W.A. Little, J. Am. Chem. Soc., 109 (1987) 4606.
20 W. Bruns and W. Kaim, J. Organomet. Chem., 390 (1990) C45.
21 W. Kaim and S. Kohlmann, Inorg. Chem., 26 (1987) 68.
22 R.A. Williams, K.F. Tesh and T.P. Hanusa, J. Am. Chem. Soc., 113 (1991) 4843.
23 R. Khattar, C. Knobler and M.F. Hawthorne, J. Am. Chem. Soc., 112 (1990) 4962.
24 M.H. Chisholm, K. Folting and J.C. Huffman, Inorg. Chem., 23 (1984) 1021.
25 J. Baumgarten, C. Bessenbacher, W. Kaim and T. Stahl, J. Am. Chem. Soc., 111 (1989) 2126.
26 L. Pauling, The Nature of the Chemical Bond, Cornell University Press, Ithaca, NY, 1960, pp. 260, 261.
27 R.D. Shannon, Acta Crystallogr., Sect. A, 32 (1976) 751.
28 S.C. Sockwell and T.P. Hanusa, Inorg. Chem., 29 (1990) 76.
29 G. de With, S. Harkema and D. Feil, Acta Crystallogr., Sect. B, 32 (1976) 3178.
30 B.N. Meyer, J.N. Ishley, A.V. Fratini and H.C. Knachel, Inorg. Chem., 19 (1980) 2324.
31 U. Fürholz, S. Joss, H.B. Bürgi and A. Ludi, Inorg. Chem., 24 (1985) 943.